Development of a chronic focal equine arteritis virus infection of a male reproductive tract cell line

Lydie Martín-Faivre, Delphine Gaudaire, Claire Laugier, Hélène Bouraïma-Lelong, Stéphan Zientara, Aymeric Hans

▶ **To cite this version:**

Lydie Martín-Faivre, Delphine Gaudaire, Claire Laugier, Hélène Bouraïma-Lelong, Stéphan Zientara, et al.. Development of a chronic focal equine arteritis virus infection of a male reproductive tract cell line. Journal of Virological Methods, 2023, 319, pp.114756. 10.1016/j.jviromet.2023.114756 . anses-04138666

HAL Id: anses-04138666

https://anses.hal.science/anses-04138666

Submitted on 3 Nov 2023

HAL is a multi-disciplinary open access archive for the deposit and dissemination of scientific research documents, whether they are published or not. The documents may come from teaching and research institutions in France or abroad, or from public or private research centers.

L'archive ouverte pluridisciplinaire **HAL**, est destinée au dépôt et à la diffusion de documents scientifiques de niveau recherche, publiés ou non, émanant des établissements d'enseignement et de recherche français ou étrangers, des laboratoires publics ou privés.

Distributed under a Creative Commons Attribution - NonCommercial - NoDerivatives 4.0 International License

Journal of Virological Methods 319 (2023) 114756

Contents lists available at ScienceDirect

Journal of Virological Methods

journal homepage: www.elsevier.com/locate/jviromet

Development of a chronic focal equine arteritis virus infection of a male reproductive tract cell line

Lydie Martín-Faivre [a,*], Delphine Gaudaire [a], Claire Laugier [a], Hélène Bouraïma-Lelong [b], Stéphan Zientara [c], Aymeric Hans [a]

[a] ANSES Laboratory for Animal Health, Normandy site. PhEED Unit, Goustranville, France
[b] Normandie Université, UNICAEN, INRA, OeReCa, 14000 Caen, France
[c] Université Paris-Est, ANSES, Maisons-Alfort Laboratory for Animal Health, UMR Virology ANSES, INRAE, ENVA, Maisons-Alfort, France

ARTICLE INFO

Keywords:
Equine arteritis virus
Viral persistence
Chronic focal infection
Horse
TM3 cells

ABSTRACT

Equine arteritis virus (EAV) is an *Alphaarterivirus* (family *Arteriviridae*, order *Nidovirales*) that frequently causes an influenza-like illness in adult horses, but can also cause the abortions in mares and death of newborn foals. Once primary infection has been established, EAV can persist in the reproductive tract of some stallions. However, the mechanisms enabling this persistence, which depends on testosterone, remain largely unknown. We aimed to establish an *in vitro* model of non-cytopathic EAV infection to study viral persistence. In this work, we infected several cell lines originating from the male reproductive tract of different species. EAV infection was fully cytopathic for 92BR (donkey cells) and DDT1 MF-2 (hamster cells) cells, and less cytopathic for PC-3 cells (human cells); ST cells (porcine cells) seemed to eliminate the virus; LNCaP (human cells) and GC-1 spg (murine cells) cells were not permissive to EAV infection; finally, TM3 cells (murine cells) were permissive to EAV infection without any overt cytopathic effects. Infected TM3 cells can be maintained at least 7 days in culture without any subculture. They can also be subcultured over 39 days (subculturing them at 1:2 the first time at 5 dpi and then every 2–3 days), but in this case, the percentage of infected cells remains low. Infected TM3 cells may therefore provide a new model to study the host-pathogen interactions and to help determine the mechanisms involved in EAV persistence in stallion reproductive tract.

1. Introduction

Equine arteritis virus (EAV) is an *Alphaarterivirus* (subfamily *Equarterivirinae*, family *Arteriviridae*, order *Nidovirales* — which also contains the *Coronaviridae* family) (Siddell et al., 2019) that was isolated for the first time in Ohio (USA) in 1953. This virus is a 40–70 nm diameter enveloped positive-strand RNA virus, which can be transmitted by the respiratory, venereal, and congenital routes (Balasuriya et al., 2013; Carossino et al., 2017; Metz et al., 2014; Pronost et al., 2010).

EAV is responsible for equine viral arteritis (EVA), a viral disease affecting equids, and whose clinical signs, during primo-infection, depend not only on the virulence of the strain, the path of infection, and the dose of challenged viruses, but also on the age and the health status of the infected animal (Balasuriya et al., 2013). The most commonly encountered clinical signs include pyrexia, depression, oedema (ventral trunk, limbs, or scrotum), conjunctivitis, nasal discharge, and leukopenia (Carossino et al., 2017; Metz et al., 2014; Pronost et al., 2010; Wada et al., 1996). However, EAV can cause transitory infertility in stallions, fatal fulminating interstitial pneumonia in newborn foals (Balasuriya et al., 2013; Pronost et al., 2010), and a progressive pneumo-enteric syndrome in 1- to 6-month-old foals (Golnik et al., 1981; Metz et al., 2014). EAV can also cause abortion in 10–70% of pregnant mares (from 3 to 10 months of gestation) (Balasuriya et al., 2013; Metz et al., 2014; Pronost et al., 2010; Wada et al., 1996).

Once the horse is infected, the virus is either eliminated within 28–34 days or, in some stallions, persists in the epididymis and in the accessory glands (Carossino et al., 2017; Holyoak et al., 1993; Neu et al., 1988). The virus is predominantly found in the ampullae of the vasa

Abbreviations: AR, androgen receptor; CK, chemokine; CPE, cytopathic effects; dpi, day(s) post-infection; EAV, equine arteritis virus; FCS, foetal calf serum; IFN, interferon; MOI, multiplicity of infection; PBST, 1X PBS containing 0.1% Triton™ X-100; PBSTB, 1X PBS containing 0.1% Triton™ X-100 and 1% bovine serum albumin; PFU, plaque-forming units; SD, standard deviation; SE, standard error.

* Correspondence to: INSERM U1152, Physiopathologie et épidémiologie des maladies respiratoires, Université Paris Cité, Paris, France.
E-mail address: lydie.martin@inserm.fr (L. Martín-Faivre).

https://doi.org/10.1016/j.jviromet.2023.114756
Received 27 March 2023; Received in revised form 8 May 2023; Accepted 27 May 2023
Available online 1 June 2023
0166-0934/© 2023 The Authors. Published by Elsevier B.V. This is an open access article under the CC BY-NC-ND license (http://creativecommons.org/licenses/by-nc-nd/4.0/).

deferentia, but it can also be found elsewhere in the vasa deferentia, the prostate, the bulbourethral glands, the epididymis, and the seminal vesicles; it can also be found in the urinary bladder and the distal urethra (Carossino et al., 2017; Holyoak et al., 1993; Neu et al., 1988). In cases of viral persistence, stallions exhibit no clinical signs, but still shed the virus in their semen and are therefore called shedder stallions. These stallions can thus propagate the virus when they are used for reproduction (Metz et al., 2014; Pronost et al., 2010).

Although the persistence of the virus in stallions has been well documented, the mechanisms involved in this viral persistence remain largely unknown. However, recent studies have suggested that persistent EAV infection in stallions is associated with an allele of the *CXCL16* gene (Carossino et al., 2019; Sarkar et al., 2016). Interestingly, CXCL16S expression, which is responsible for T cell susceptibility to EAV infection, is neither necessary nor sufficient for EAV persistence in stallions. One study (Sarkar et al., 2016) showed that 25% of stallions (11/43) expressing the CXCL16S protein do not exhibit long-term EAV persistence. On the other hand, 14% of stallions (5/34) homozygous for the CXCL16 protein resistance genotype did show long-term EAV persistence. These data indicate that genetic susceptibility alone cannot explain EAV persistence in stallions. Interestingly, it has been shown that, following castration, the virus is no longer detected in the semen and the accessory sex glands of shedder stallions (Holyoak et al., 1993; Little et al., 1992; McCollum et al., 1994). In castrated stallions that are supplemented with testosterone at a physiological concentration, viral persistence does remain (Holyoak et al., 1993; Little et al., 1992; McCollum et al., 1994). Moreover, other studies have demonstrated that anti-GnRH vaccines, which suppress the synthesis of numerous hormones including testosterone (Janett et al., 2009; Stout, 2005), can clear EAV from the semen of shedder stallions (Burger et al., 2006; Stout, 2005). However, their effectiveness varies with individual stallions (Burger et al., 2006; Janett et al., 2009; Stout, 2005). Taken together, these results suggest a predominant role of testosterone in EAV persistence in the stallion reproductive tract.

Thus, understanding the mechanisms behind EAV persistence in the stallion reproductive tract is of major importance for developing innovative treatments to eliminate EAV in persistently infected stallions.

Unlike other *Arteriviridae*, EAV is able to infect, *in vitro,* primary cell cultures from several different species as well as different cell lines, such as equine cells (dermal cells [E. Derm, also called NBL-6], endothelial cells [EEC]), hamster cells (lung cells [HmLu], kidney cells [BHK-21]), human cervix cells (HeLa), rabbit kidney cells (RK13), and monkey kidney cells (Vero, JINET, LLC-MK2, and MARC-145) (Fukunaga et al., 1984; Golnik et al., 1981; Konishi et al., 1975; Lu et al., 2012; Zhang et al., 2008). However, EAV cannot infect non-equid animals and no *in vitro* model of persistently EAV-infected cells from the male reproductive tract has been described yet. The aim of this work was to establish an *in vitro* model of EAV infection in cells from the male reproductive tract that express the androgen receptor to enable the study of the mechanisms involved in EAV persistence in stallions.

2. Materials and methods

2.1. Cell culture conditions

Seven cell lines (described in Table 1) were tested: 92BR, DDT1 MF-2, ST, PC-3, TM3, GC-1 spg, and LNCaP cells. The rabbit kidney cell line (RK13), highly permissive to EAV, is recommended by the World Organisation for Animal Health (OIE) to reveal the presence of EAV in stallion semen and to amplify the virus, and was used as a positive control for EAV infection. The cell culture media of all cell lines were supplemented with 50 units/mL penicillin and 50 μg/mL streptomycin (Gibco, Invitrogen), and 25 mM HEPES (Gibco, Invitrogen) for RK13, 92BR, DDT1 MF-2, ST, PC-3, and GC-1 spg cells, or 15 mM HEPES (Gibco, Invitrogen) for TM3 cells. Moreover, 1 mM sodium pyruvate (Gibco, Invitrogen) was added to the culture media for RK13, 92BR, ST, PC-3, and GC-1 spg cells, and 0.5 mM for TM3 cells. RK13, 92BR, and ST cells were grown in Eagle's minimum essential medium (MEM) (Gibco, Invitrogen) supplemented with 1X non-essential amino acids (NEAA) (Gibco, Invitrogen), and either 10% heat-inactivated foetal calf serum (FCS) (Gibco, Invitrogen) for RK13 and ST cells, or 15% heat-inactivated FCS (Gibco, Invitrogen) for 92BR cells. DDT1 MF-2 and GC-1 spg cells were grown in Dulbecco's modified Eagle's medium (DMEM) (Gibco, Invitrogen) supplemented with, respectively, 5% and 10% heat-inactivated FCS (Gibco, Invitrogen). TM3 cells were grown in DMEM: Ham's F-12 nutrient mixture (DMEM/F-12) (Gibco, Invitrogen) medium supplemented with 5% heat-inactivated horse serum (Dominique Dutscher) and 2.5% heat-inactivated FCS (Gibco, Invitrogen). LNCaP cells were grown in Roswell Park Memorial Institute (RPMI) (Gibco, Invitrogen) medium supplemented with 10% heat-inactivated FCS (Gibco, Invitrogen). PC-3 cells were cultured in Ham's F-12K (Kaighn's) (Gibco, Invitrogen) medium supplemented with 10% heat-inactivated FCS (Gibco, Invitrogen). All cell lines were maintained at 37 °C in a humid atmosphere with 5% CO_2.

2.2. Viral infection

The Bucyrus strain of EAV (ATCC® VR-796™) was used for cell infections. 92BR, DDT1 MF-2, ST, PC-3, TM3, GC-1 spg, and LNCaP cells were infected in suspension with a multiplicity of infection (MOI) of 10 to avoid overlooking low permissive cell lines, whereas RK13 cells, already known to be highly permissive to EAV, were infected at an MOI of 1, except for the plaque assays, described in subsection 2.3. The infected suspensions were pre-incubated in 15 mL Falcon® tubes for 1 h with 2 mL of medium at 37 °C in a humid atmosphere with 5% CO_2, to help promote contact of the virus with the cells. Mock-infected cells

Table 1
Cell lines tested in this study.

Cell line	Source	Cell type	Morphology	Androgen receptor expression
RK13	ATCC® CCL-37™	rabbit kidney	epithelial	negative (Shin et al., 2009)
92BR	HPA 90011874	donkey testis	fibroblast	not described
DDT1 MF-2	ATCC® CRL-1701™	leiomyosarcoma of the ductus deferens of a Syrian golden hamster	epithelial	positive (characterized by the supplier)
ST	ATCC® CRL-1746™	porcine testis (immature Sertoli cells)	fibroblast	positive (Ma et al., 2016)
PC-3	ATCC® CRL-1435™	human prostate adenocarcinoma cells derived from a metastatic site: bone	epithelial	positive, but androgen non-responsive (Alimirah et al., 2006)
TM3	ATCC® CRL-1714™	murine immature Leydig cells	epithelial	positive (characterized by the supplier)
GC-1 spg	ATCC® CRL-2053™	murine immortalized type B spermatogonia	epithelial	positive (Wang et al., 2021)
LNCaP (Clone FGC)	ATCC® CRL-1740™	human prostate carcinoma cells derived from a metastatic site: left supraclavicular lymph node	epithelial	positive (characterized by the supplier)

were inoculated with RK13 cell culture medium without virus. Cells were then seeded in plates, culture slides, or flasks.

Once the cells adhered to the plastic, usually after 4–5 h, cell culture media were replaced with fresh media, except for LNCaP cells. For immunofluorescence staining on slides, media were not replaced.

2.3. Plaque assays

Preformed confluent cell monolayers of the different tested cell lines, grown in 6-well plates, were inoculated with 10-fold serial dilutions of EAV (10^{-1} to 10^{-8}): the EAV Bucyrus strain (ATCC® VR-796™) was used to test the lytic effect of EAV on these cell lines.

To study EAV replication and production of infectious viral particles, assays were performed in 6-well plates with 8×10^5 cells per well. Cells were infected as described in subsection 2.2. Supernatants of the cell lines were harvested at 1, 2, and 3 days post-infection (dpi) and their infectivity was assessed using plaque assays on preformed RK13 cell monolayers.

In both experiments, the inoculum was removed 4 h later and replaced with fresh culture medium, reduced in serum (1:5), containing 0.75% carboxymethylcellulose. At 3 dpi, the cell monolayers were stained with a 0.2% formalin-buffered crystal violet solution to visualize cytopathic effects (CPE).

2.4. Cell survival assays

For cell survival assays, 2×10^4 cells per well (4 replicates for each condition) were seeded in 96-well plates. Cell viability was assessed using a luciferase-based viability assay, which evaluates the number of living cells in culture, based on the quantification of ATP present in the cell culture (CellTiter-Glo®; Promega). Briefly, in presence of ATP and oxygen, luciferase oxidizes luciferin into a luminescent form. The generated luminescence signal is proportional to the number of metabolically active cells. ATP was quantified in control wells containing either mock-infected cells or dead cells, after cell lysis with IGEPAL (Sigma) diluted to 1:400. Before ATP quantification, the plate was equilibrated at room temperature for 30 min. Half of the culture medium was removed from each well and replaced by an equal volume of CellTiter-Glo®. Plates were incubated for another 30 min at room temperature under continuous gentle shaking (50 rpm). Lysates were analysed with the TECAN Infinite® F200 PRO multimode microplate reader. Luminescence was recorded for 1 s without attenuation.

2.5. Immunofluorescence staining on slides

For immunofluorescence staining on slides, 5×10^4 cells per well were seeded in Falcon® 8-well culture slides. The following antibodies were used: a monoclonal antibody specifically recognizing the nucleocapsid protein (N) of the Bucyrus strain of EAV (VMRD, cat no 17D3, mouse IgG1, 1:500 dilution), a monoclonal Alexa Fluor® 647-labeled antibody raised against tubulin (Abcam, clone YOL1/34, rat monoclonal IgG2a, 1:100 dilution). The Dylight® 488-conjugated goat anti-mouse IgG secondary antibody was from Thermo-Scientific (cat no 35503, 1:200 dilution). The non-specific binding of the anti-N antibody and the secondary antibody was evaluated on mock-infected cells.

Cells were fixed with cold 4% formaldehyde for 30 min at room temperature and permeabilized with a cold solution of methanol: acetone (50:50) for 10 min at room temperature. Cells were then washed twice with 1X PBS containing 0.1% Triton™ X-100 (PBST). Cells were incubated with the anti-N antibody for 1 h at room temperature, then with the secondary antibody for 1 h at room temperature, and finally with the anti-tubulin antibody overnight at 4 °C. After each incubation step, cells were washed three times for 5 min with PBST. Coverslips were mounted with Vectashield® mounting medium for fluorescence with DAPI H-1200 (Vector Laboratories, Burlingame, CA) to stain DNA. Slides were analysed by fluorescence microscopy using an EVOS® FL Cell Imaging System (Life technologies).

2.6. Immunofluorescence staining for flow cytometry

For flow cytometry analyses, 2×10^6 cells per T25 flask were seeded for DDT1 MF-2, ST, PC-3, TM3, GC-1 spg, and LNCaP cells, and 3×10^6 cells per T75 flask were seeded for RK13 and 92BR cells. For the EAV dissemination study, the media of TM3 and PC-3 cell cultures were changed after the third day of culture.

Cells were dissociated, then fixed in 4% formaldehyde for 30 min at 4 °C. A maximum of 10^6 cells were pelleted by centrifugation at 240 *g* for 3 min at 4 °C, then resuspended and permeabilized for 10 min on ice with a cold solution of methanol:acetone (50:50). Then, 1X PBS containing 0.1% Triton™ X-100 and 1% bovine serum albumin (PBSTB) was added, and cells were centrifuged for 3 min at 240 *g* at 4 °C. Cells were then washed in PBSTB and centrifuged as described above. After blocking with PBSTB for 20 min on ice, cells were incubated with the anti-N antibody (described in the subsection 2.5) for 30 min on ice. Cells were then washed twice in PBSTB and centrifuged for 5 min at 835 *g* at 4 °C, before being incubated for 30 min on ice with the secondary antibody described in the subsection 2.5. Cells were then washed twice in PBSTB and resuspended in 2% formaldehyde. Samples were processed by a Gallios flow cytometer (Beckman Coulter) and the results were analysed using the Kaluza software (Beckman Coulter).

2.7. Preparation of viral RNA and RT-qPCR analysis

To study EAV replication, assays were performed in 6-well plates with 8×10^5 cells per well. For relative gene expression assays of alpha and beta interferons (IFN-α and IFN-β) in TM3 cells, 2×10^6 cells per T25 flask were seeded.

RNAs were extracted from cells as follows. Cell monolayers in 6-well plates and T25 flasks were first lysed with, respectively, 1 mL and 2.5 mL of TRIzol (Ambion). RNA extractions were performed on 500 μL of sample to which 100 μL of chloroform was added. The mix was vortexed for 3 min, left 3 min at room temperature, and then centrifuged at 12000 *g* for 15 min at 4 °C. The aqueous phase was recovered, approximately 200 μL, to which 300 μL of 70% ethanol was added. This mix underwent RNA extraction using the RNeasy® Mini Kit (Qiagen) as recommended by the manufacturer, with on-column DNase digestion with 5 units of Turbo DNAse™ (Ambion) to remove genomic DNA. A second elution step was performed to recover RNA from the cells.

Cell supernatant was centrifuged at 835 *g* for 10 min to eliminate dead cells. RNA extraction was performed on 140 μL of centrifuged supernatant with the QIAamp® Viral RNA kit (Qiagen), according to the manufacturer's instructions (a second elution step was carried out).

The detection of the EAV genome was performed using RT-qPCR with the QuantiTect™ Virus + ROX Vial Kit (Qiagen). Primer and probe sequences used for ORF7 gene amplification were from Balasuriya et al. (2002). A set of copies of the EAV genome was used to quantify the number of genome copies in the samples. To obtain this set of copies of the EAV genome, a plasmid containing the ORF7 gene was transcribed into RNA with T3 RNA polymerase (Thermo Scientific) according to the manufacturer's instructions. Data were acquired in triplicate on a MasterCycler realplex^4 epgradient S (Eppendorf, Hamburg, Germany). Cycling conditions were as follows: 20 min at 50 °C, 5 min at 95 °C, and 45 cycles of 15 s at 95 °C followed by 45 s at 60 °C. The quantity of intracellular viral RNA was normalized to the quantity of total RNA (measured using a Nanodrop 2000c spectrophotometer, Thermo Scientific).

IFN-α and IFN-β gene expression was evaluated using RT-qPCR with the QuantiFast® SYBR® Green RT-PCR kit (Qiagen). Primer sequences used are described in Table 2 and were from Wu et al. (2016) (used on Leydig, Sertoli, and male germ cells), except for the housekeeping gene sequences, whose primers are described in Li et al. (2012) and Shen et al. (2012) (used on Leydig and TM3 cells, respectively). The β-actin and

Table 2
Primers and probe used in this study.

Target gene	Type	Sequence	Concentration used
EAV ORF7	Forward primer	5′-GGCGACAGCCTACAAGCTACA-3′	0.4 μM
EAV ORF7	Reverse primer	5′-CGGCATCTGCAGTGAGTGA-3′	0.4 μM
EAV ORF7	Probe	[6FAM]-TTGCGGACCCGCATCTGACCAA-[TAM]	0.2 μM
IFN-α	Forward primer	5′-TTCCTCAGACTCATAACCTCAGGA-3′	0.6 μM
IFN-α	Reverse primer	5′-ATTTGTACCAGGAGTGTCAAGGC-3′	0.6 μM
IFN-β	Forward primer	5′-GACGTGGGAGATGTCCTCAAC-3′	0.75 μM
IFN-β	Reverse primer	5′-GGTACCTTTGCACCCTCCAGTA-3′	0.75 μM
β-actin-TM3	Forward primer	5′-TCTGGCACCACACCTTCTA-3′	1 μM
β-actin-TM3	Reverse primer	5′-AGGCATACAGGGACAGCAC-3′	1 μM
GAPDH	Forward primer	5′-CCAGGTTGTCTCCTGCGACTTCA-3′	1 μM
GAPDH	Reverse primer	5′-GGGTGGTCCAGGGTTTCTTACTCC-3′	1 μM

GAPDH genes were used as internal quantitative controls for the amplification. Moreover, β-actin was used for gene expression normalization. Samples were processed in triplicate and data were acquired with a LightCycler® 480 II (Roche, Germany). Cycling conditions were as follows: retrotranscription for 10 min at 50 °C, HotStarTaq *Plus* DNA polymerase activation for 5 min at 95 °C, and 45 cycles of 10 s at 95 °C followed by 30 s at 60 °C. Data were analysed using the $2^{-\Delta\Delta Ct}$ method with $\Delta\Delta Ct$ = (mean of IFN gene Ct - mean of actin gene Ct)$_{\text{infected cells}}$ -(mean of IFN gene Ct - mean of actin gene Ct)$_{\text{mock-infected cells}}$.

2.8. Subcultures of EAV-infected TM3 cells

TM3 cells were infected in suspension at an MOI of 10. 2×10^6 cells were seeded in T25 flasks with complete medium and were incubated for 5 h at 37 °C with 5% CO_2. The supernatant was then removed and replaced with fresh medium. Cells were subcultured at 1:5 at 1, 2, or 3 dpi. To this end, cell monolayers were washed twice with 1X PBS and then washed with 1X PBS containing 1:10 trypsin before being detached. Then, at 1, 2, or 3 days post-subculturing, immunofluorescence staining for flow cytometry was performed as described above in subsection 2.6.

In parallel, to attempt to maintain infected TM3 cells in culture, they were subcultured several times at 1:2, 1:5, 1:10, 1:20, or 1:100, every 1–6 days of culture.

2.9. Statistical analysis

Data are expressed as mean +/- standard error (SE) for cell survival assays, or +/- standard deviation (SD) for immunofluorescence staining for flow cytometry, the quantification of EAV replication, and the quantification of infectious viral particle production. For the quantification of EAV replication and of the infectious viral particle production, two-tailed unpaired Student's *t*-tests were carried out to compare the cell lines when indicated.

For cell survival assays, when data were normalized to the results of mock-infected cells, the statistical significance of the results was evaluated using a one-tailed one-sample Student's *t*-test: infected cell results were compared with the theoretical mean of 100% (mean based on mock-infected cells). When data were normalized to the results obtained at 1 dpi, the statistical significance of the results was evaluated using a one-tailed paired Student's *t*-test.

Correlations between the percentage of infected cells and the number of viral genome copies, and between the percentage of infected cells and type I interferon gene expression, were assessed using a one-tailed Pearson's correlation test.

3. Results

3.1. Cell line permissiveness to EAV infection

To assess the permissiveness of the different cell lines to EAV infection, preformed confluent cell monolayers of each cell line were incubated with 10-fold serial dilutions of EAV Bucyrus strain to distinguish between permissive, low permissive, and non-permissive cell lines. The plaque assays performed with highly permissive cells, such as RK13 cells, showed CPE at 3 dpi. The same pattern was found for 92BR and DDT1 MF-2 cells, with cell monolayers totally destroyed respectively at dilutions 10^{-4}, 10^{-3}, and 10^{-2} of an EAV Bucyrus solution (Fig. 1A). Plaque-forming units (PFU) were detectable from a 10^{-5} dilution for RK13 cells, from 10^{-4} to 10^{-6} dilutions for 92BR cells, and from 10^{-3} to 10^{-6} dilutions for DDT1 MF-2 cells (Fig. 1A). CPE was weaker in ST cells, with tiny plaques on cell monolayers after 3 dpi with the EAV Bucyrus solution diluted to 1:10 (10^{-1}) (Fig. 1B). The last group of cell lines tested, including PC-3, TM3, GC-1 spg, and LNCaP cells, did not exhibit any CPE on cell monolayers at 3 dpi regardless of the EAV Bucyrus concentration used (Fig. 1A, B, and data not shown).

In addition to plaque assays, CPE associated with EAV infection was quantified at 1 and 3 dpi by measuring cell survival using a luciferase-based viability assay that relied on ATP quantification. Cell viability assessed at 3 dpi in RK13 cells infected at an MOI of 1 or 10 (data not shown) revealed a cell survival rate of approximately 7% (Fig. 1C). This survival rate reached around 43% and 12% for the DDT1 MF-2 and 92BR cell lines infected at an MOI of 10, respectively (Fig. 1C), and confirmed the results obtained by plaque assays. The survival rates recorded for GC-1 spg, LNCaP, and ST cells, infected at an MOI of 10, revealed that no cell death was associated with EAV infection (Fig. 1C). Although no PFUs were observed in plaque assays for TM3 and PC-3 cells, the cell survival assay indicated that EAV infection may cause cell death or slow down cell growth, because survival rates recorded at 3 dpi were around 89% and 69% in TM3 and PC-3 cells, respectively.

To better characterize EAV infection in the different cell lines, immunofluorescent staining with monoclonal antibodies was used to detect the viral N protein and tubulin. Viral protein expression was detected as early as 1 dpi in RK13, 92BR, DDT1 MF-2, ST, PC-3, and TM3 cells, but not in GC-1 spg and LNCaP cells (Fig. 2A). Moreover, N protein expression was still detectable after 3 dpi in RK13, 92BR, DDT1 MF-2, PC-3, and TM3 cells, but not in ST cells, and remained undetectable in GC-1 spg and LNCaP cells (Fig. 2B). Flow cytometry experiments confirmed that more than 90% of RK13 and 92BR infected cells expressed the viral N protein as of 1 dpi (Fig. 2C). Conversely, only 6% of the infected DDT1 MF-2 cells expressed the N protein at 1 dpi. However, the viral infection spread rather quickly to reach around 85% of infected cells at 3 dpi (Fig. 2C). Similarly to DDT1 MF-2 cells, only 2% and 3.2% of PC-3 and TM3 cells were infected at 1 dpi, respectively. Viral spreading also occurred in these two cell lines with 24% and 31.5% of PC-3 and TM3 cells, respectively, infected at 3 dpi without overt CPE (Fig. 2C). Surprisingly, no infected cells were detected with flow cytometry in the ST cell line neither at 1 dpi nor at 3 dpi (Fig. 2C). No infected cells were revealed by flow cytometry for LNCaP and GC-1 spg cells following EAV infection (Fig. 2C).

3.2. EAV replication and production of infectious viral particles in the different cell lines

EAV replication was evaluated by measuring the viral genome copy number produced in the supernatant as well as within the infected cell lines following EAV infection (Fig. 3A and C). The EAV genome copy number measured in the supernatant of RK13 and 92BR cells increased

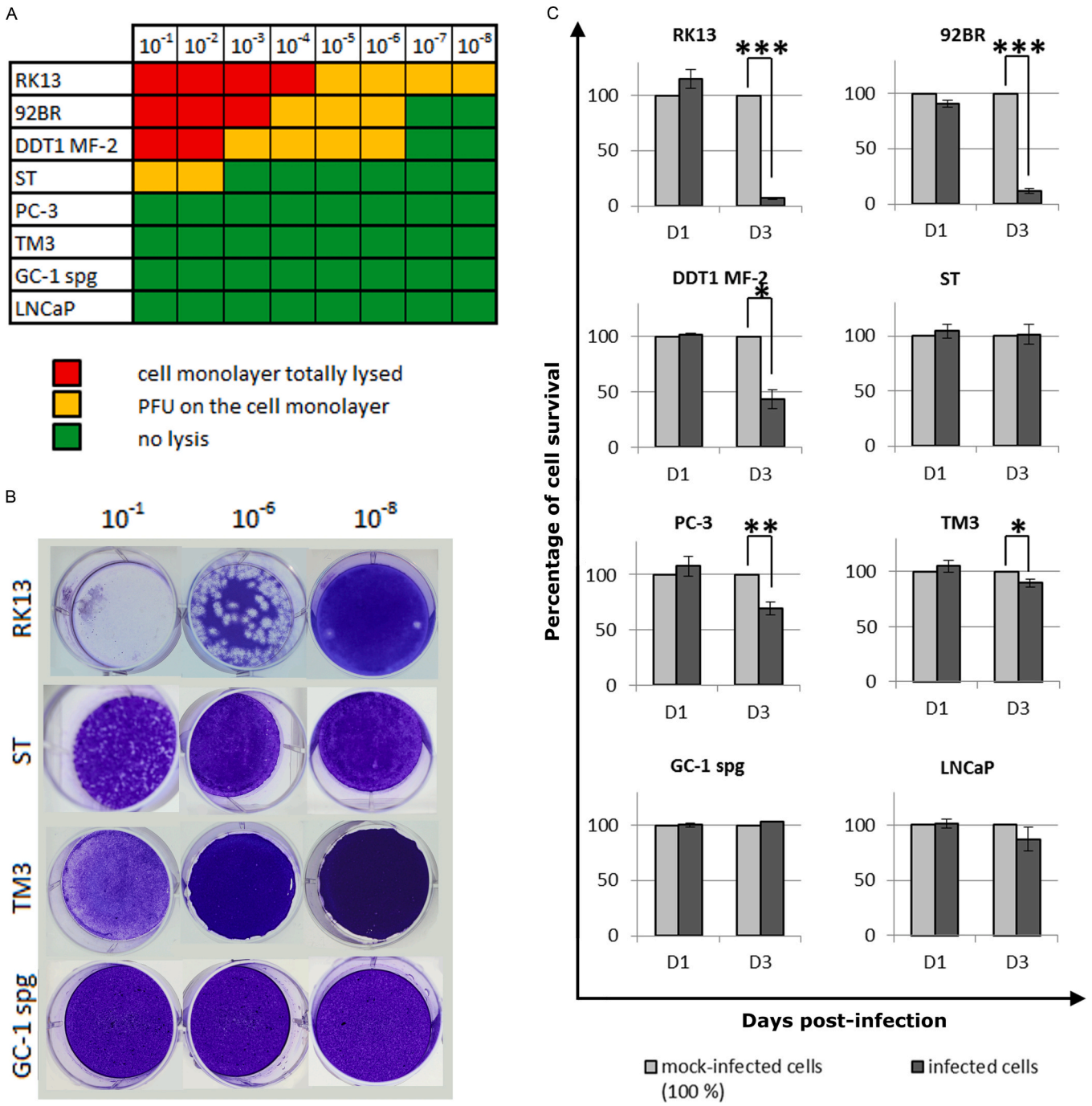

Fig. 1. Determination of the lytic effect of EAV on different cell lines. (A) Representative results of plaque assays performed with serial dilutions of EAV. (B) Photos of representative cell monolayer patterns obtained during plaque assays performed with EAV serial dilutions. (C) CellTiter-Glo® assays. The RK13 cell line was infected at an MOI of 1. The other cell lines were infected at an MOI of 10. After 1 and 3 dpi (D1 and D3, respectively), the luminescence signal obtained was normalized to the luminescence signal obtained for the mock-infected cells. Results are from 3 to 7 independent experiments (mean +/- SE). A one-tailed one-sample Student's *t*-test compared the infected cell results to the theoretic mean of 100% (mean of mock-infected cells). * $p < 0.05$, ** $p < 0.01$, *** $p < 0.001$.

as early as 1 dpi to reach a maximum of approximately 10^{11} genome copies per mL of supernatant for a period of 3 days (Fig. 3A). These two cell lines also exhibited the same amount of EAV genome copies within the cells (~10^7-10^8 genome copies/ng total RNA) between 1 and 3 dpi (Fig. 3C). At 1 dpi, DDT1 MF-2, ST, PC-3, and TM3 cells produced between 10^8 and 10^9 EAV genome copies per mL of supernatant, and 10^5 to 10^6 EAV genome copies per ng of RNA within cells (Fig. 3A and C). Interestingly, at 1 dpi, the number of viral genome copies detected within infected TM3 cells was 10-fold higher than those detected within PC-3 and DDT1 MF-2 cells (Fig. 3C) ($p = 0.0390$ and $p = 0.0475$, respectively), whereas these cell lines exhibited a weak percentage of infection: 3.2%, 2%, and 6.4%, respectively (Fig. 2C). At 3 dpi, infected DDT1 MF-2 cells produced as many viral genome copies in the supernatant and within cells as RK13 and 92BR cells (Fig. 3A and C). This viral genome detection seemed correlated with the percentage of infected cells. Indeed, only 6% of DDT1 MF-2 cells were infected at 1 dpi, compared with 90% for RK13 and 92BR cells. This percentage was around 85% for the RK13, 92BR, and DDT1 MF-2 cell lines at 3 dpi. Pearson's correlation coefficients between the percentage of infected cells and the viral genome copy number in the supernatant or within

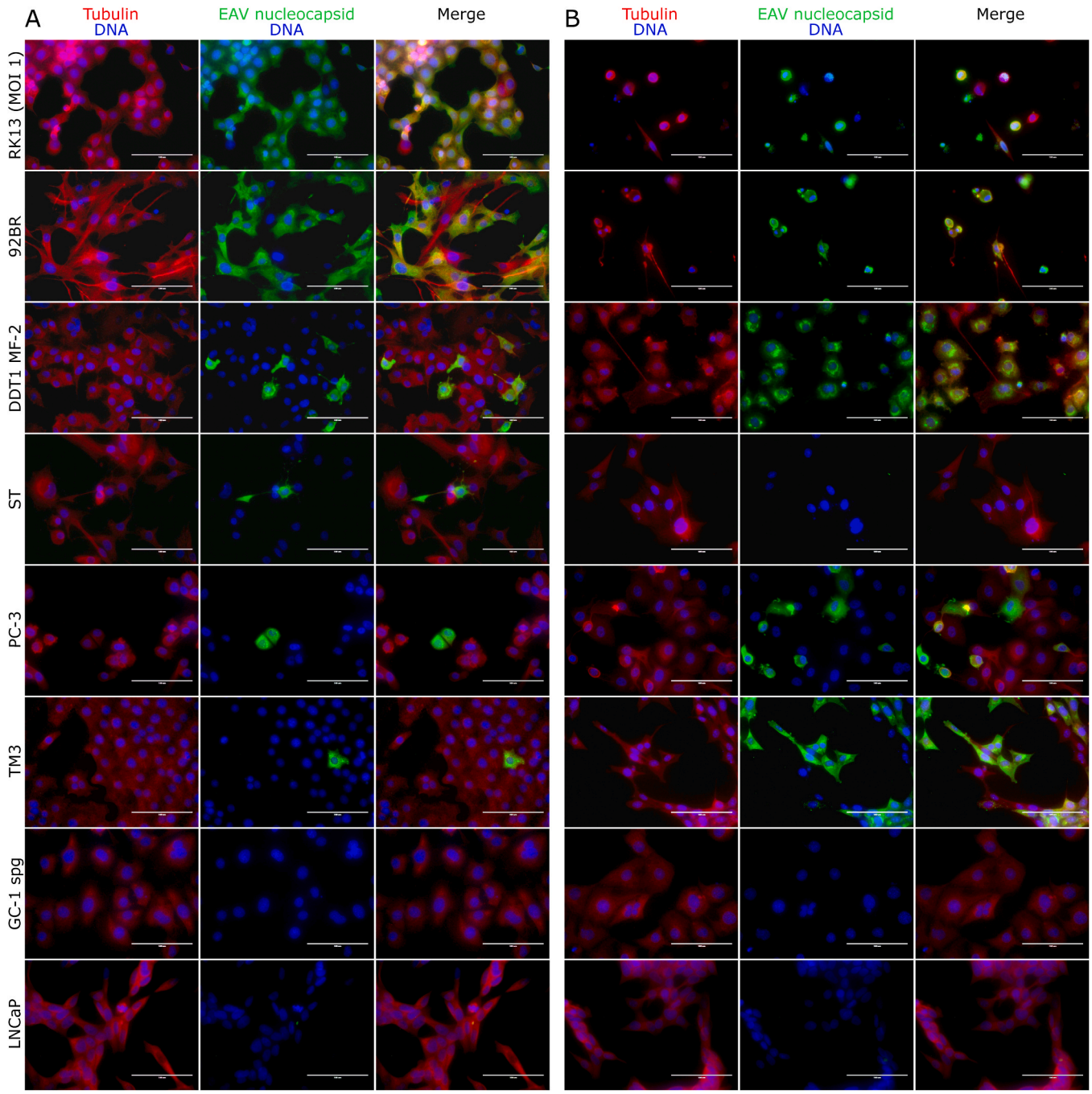

Fig. 2. Detection of the EAV nucleocapsid protein (N) in infected cells. (A and B) Representative images of immunofluorescence staining on slides after 1 dpi (A) and 3 dpi (B). The RK13 cell line was infected at an MOI of 1 and the other cell lines were infected at an MOI of 10. The colour code used is shown. Scale bars represent 100 μm. (C) Percentages of infected cells obtained by flow cytometry after 1 and 3 dpi (D1 and D3, respectively). The RK13 cell line was infected at an MOI of 1 and the other cell lines were infected at an MOI of 10. ND, no infected cells were detected. Results are from 2 to 5 independent experiments (n = 2 for RK13 cells, 92BR cells, GC-1 spg, and LNCaP cells, n = 3 for DDT1 MF-2 cells, n = 4 for PC-3 cells, and n = 5 for TM3 cells) (mean +/- SD).

cells were 0.9347 and 0.8419, respectively ($p < 0.0001$ and $p < 0.0001$, respectively). However, the TM3 cell line also produced a high quantity of EAV genomes with 10^{10} genome copies per mL of supernatant and 10^{7} genome copies per ng of total RNA, detected respectively in the supernatant and within the cells, at 2 dpi. At 3 dpi, TM3 cells infected at 30% produced only 10-fold fewer viral genome copies in the supernatant and within cells than RK13 cells infected at 90% ($p = 0.0609$ and $p = 0.0139$, respectively). Surprisingly, after 3 days of EAV infection, PC-3 and ST cells both produced fewer than 10^{9} copies of EAV genome per mL of supernatant, and fewer than 10^{5} EAV genome copies per ng RNA within cells, which is respectively 1 and nearly 2 $\log_{10}$ less than infected TM3 cells (Fig. 3A and C), even though this difference is not statistically significant ($p = 0.2$ and $p = 0.46$, respectively). Indeed, no EAV infection was observed in ST cells at 3 dpi using immunofluorescence staining, whereas PC-3 cells presented approximately the same percentage of infected cells as TM3 cells (Fig. 2B and C). However, this absence of infection detected with immunofluorescence in ST cells at 3 dpi can be correlated with a decrease in the number of EAV genome

C

	D1	D3
RK13 (MOI 1)	92.2 (+/-4.3) %	86.6 (+/-9.6) %
92BR	92.2 (+/-7.4) %	82.2 (+/-11.2) %
DDT1 MF-2	6.4 (+/-4.4) %	84.1 (+/-7.0) %
ST	ND	ND
PC-3	2.0 (+/-0.7) %	24.0 (+/-12.6) %
TM3	3.2 (+/-2.0) %	31.5 (+/-7.9) %
GC-1 spg	ND	ND
LNCaP	ND	ND

Fig. 2. (*continued*).

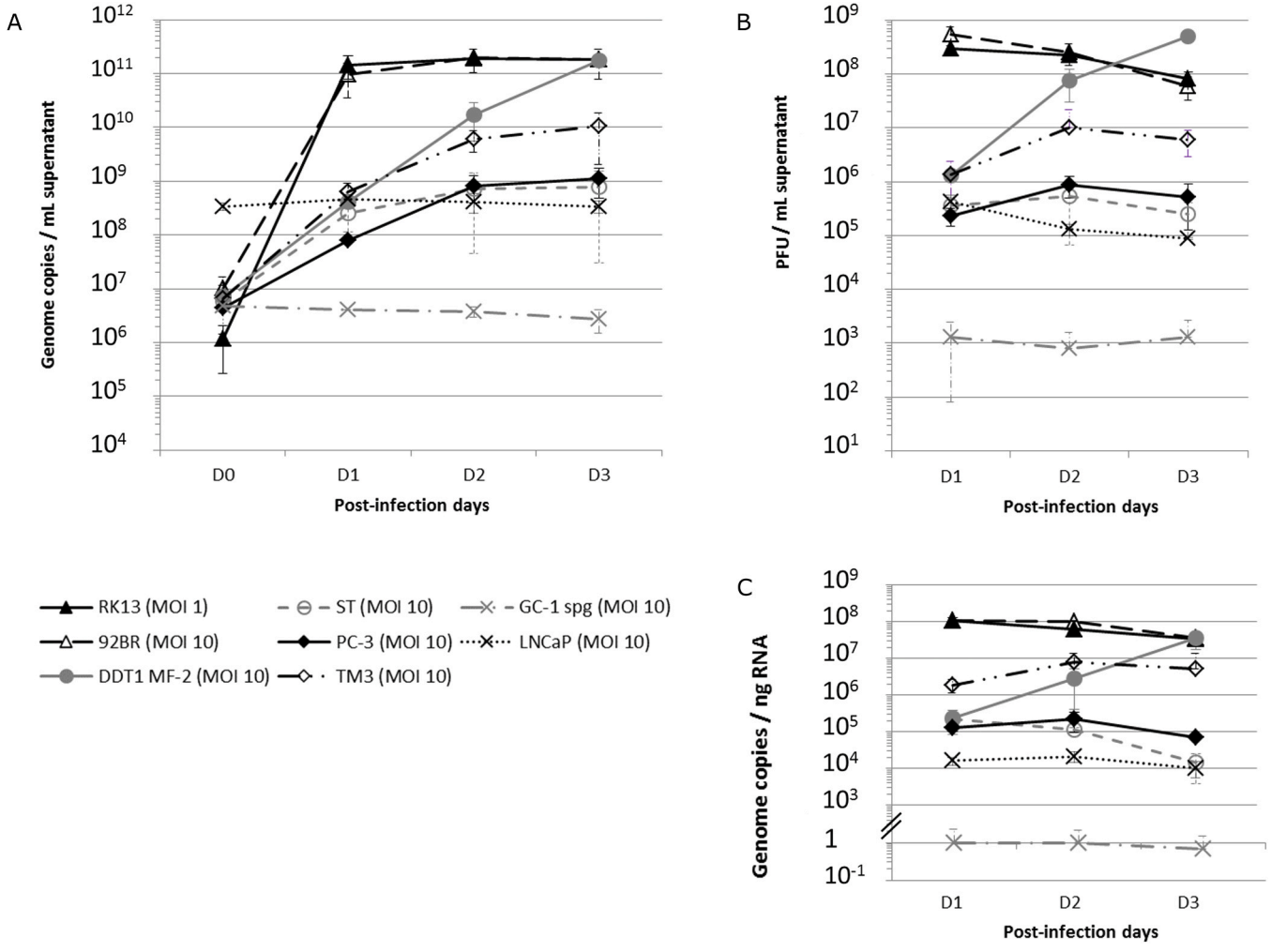

Fig. 3. EAV replication and viral production in different cell lines. (A) Quantity of EAV genome copies in the supernatant of the different cell lines tested from 0 dpi (D0) to 3 dpi (D3). Results are from 2 to 4 independent experiments (n = 2 except for LNCaP cells [n = 3] and TM3 cells [n = 4]) (mean +/- SD). (B) EAV infectious viral particles (PFU/mL) present in the supernatant of the different cell lines tested from 1 dpi (D1) to 3 dpi (D3). Results are from 2 to 4 independent experiments (n = 2 except for LNCaP cells [n = 3] and TM3 cells [n = 4]) (mean +/- SD). (C) Quantity of EAV genome copies within the cells from 1 dpi (D1) to 3 dpi (D3). Results are from 2 to 4 independent experiments (n = 2 except for TM3 cells [n = 4]) (mean +/- SD).

copies within cells since 1 dpi. Finally, no production of EAV genome copies was detected after infection of LNCaP and GC-1 spg cells, either in the supernatant or within cells (Fig. 3A and C). The number of genome copies was higher in LNCaP cell cultures than in GC-1 spg cell cultures, because the inoculum in LNCaP cell cultures could not be removed due to adherence difficulties in this cell line.

In addition to the production of viral genome copies, the release of infectious viral particles following EAV infection of the different cell lines was assessed using plaque assays on RK13 cell monolayers. Between 10^8 and 10^9 PFU per mL of supernatant were recovered at 3 dpi

from the cell culture media of the RK13, 92BR, and DDT1 MF-2 cell lines (Fig. 3B). At 3 dpi, viral production was evaluated at between 10^5 and 10^6 PFU per mL of supernatant in ST and PC-3 cells, and at around 10^7 PFU per mL of supernatant for TM3 cells (Fig. 3B) ($p = 0.0742$ and $p = 0.0651$, respectively). Conversely to viral genome copy number, the number of PFU per mL of supernatant of RK13, 92BR, and LNCaP cells decreased as early as 2 dpi (Fig. 3A and B).

In summary, GC-1 spg and LNCaP cells did not seem to be permissive to EAV infection, and EAV infection in ST cells was not detectable at 3 dpi. Infection of the 92BR and DDT1 MF-2 cell lines was cytopathic within 3 days. Only the PC-3 and TM3 cell lines were permissive to EAV infection without overt CPE at 3 dpi. Therefore, we subsequently focused on the description of PC-3 and TM3 cell infections by EAV up to 7 dpi.

3.3. Characterization of EAV infection of the PC-3 and TM3 cell lines at up to 7 days

EAV spreading was studied in PC-3 and TM3 cells up to 6 dpi, because no overt CPE was observed after 3 dpi. These two cell lines were infected at an MOI of 10, and only 2–3.2% of the cells were infected at 1 dpi (Fig. 4B) compared with 92.2% for the highly permissive RK13 cells, infected at an MOI of 1. Interestingly, the percentage of infected cells increased steadily from 1 dpi to 3 dpi to reach around 25% for PC-3 cells and around 30% for TM3 cells. Then, from 4 to 6 dpi, the proportion of infected cells decreased from around 20% to around 8% for PC-3 cells and from around 30% to around 15% for TM3 cells (Fig. 4B), whereas RK13 cells died due to the viral CPE.

To confirm our first results indicating that EAV infection did not induce a major CPE in TM3 and PC-3 cells, a growth and survival assay was performed on these two models by measuring the ATP level present in each condition over a 7-day period. The survival assay performed at 1, 2, 3, 4, and 7 dpi on RK13 cells, which are highly permissive to EAV, showed that as of 2 dpi, EAV cytopathogenic features were characterized by 74% cell death, which reached 90% at 3 dpi and more than 95% at 4 dpi and 7 dpi (Fig. 5A). Regarding PC-3 cells, EAV infection seemed to impair cell growth because at 3 dpi, a survival rate of 92 +/− 15% was recorded for infected cells compared with 157 +/− 33% for mock-infected cells (Fig. 5B). Cell death associated with EAV infection started at 4 dpi and continued until 7 dpi with recorded survival rates of 62 +/− 12% and 34 +/− 14%, respectively. Interestingly, EAV infection of TM3 cells did not modify either the cell mortality rate or cell growth, when compared with mock-infected cells over the 7-day period (Fig. 5C). However, the infection seemed to interfere slightly with cell growth at 3 dpi. These results encouraged us to pursue our study using infected TM3 cells.

3.4. EAV infection-induced interferon gene expression in TM3 cells

During the 7-day infections, TM3 cells did not present overt CPE and only 30% of the cell population was infected. We hypothesized that some antiviral molecules, such as interferons (IFN), may interfere with viral spread in the TM3 cell cultures. Thus, type I IFN (IFN-I) gene expression was assessed at 1, 2, 3, and 4 dpi. Relative gene expression of IFN-α and IFN-β in infected TM3 cells was detected at 2 dpi and reached a peak at 3 dpi. EAV infection induced a strong overexpression — up to 17-fold — of these two immune-antiviral molecules (Fig. 6A and B). The maximum IFN-α and IFN-β gene expressions at 3 dpi were correlated with the highest percentage of infected cells (Fig. 4B). Pearson's correlation coefficients between the percentage of infected cells and IFN-α or

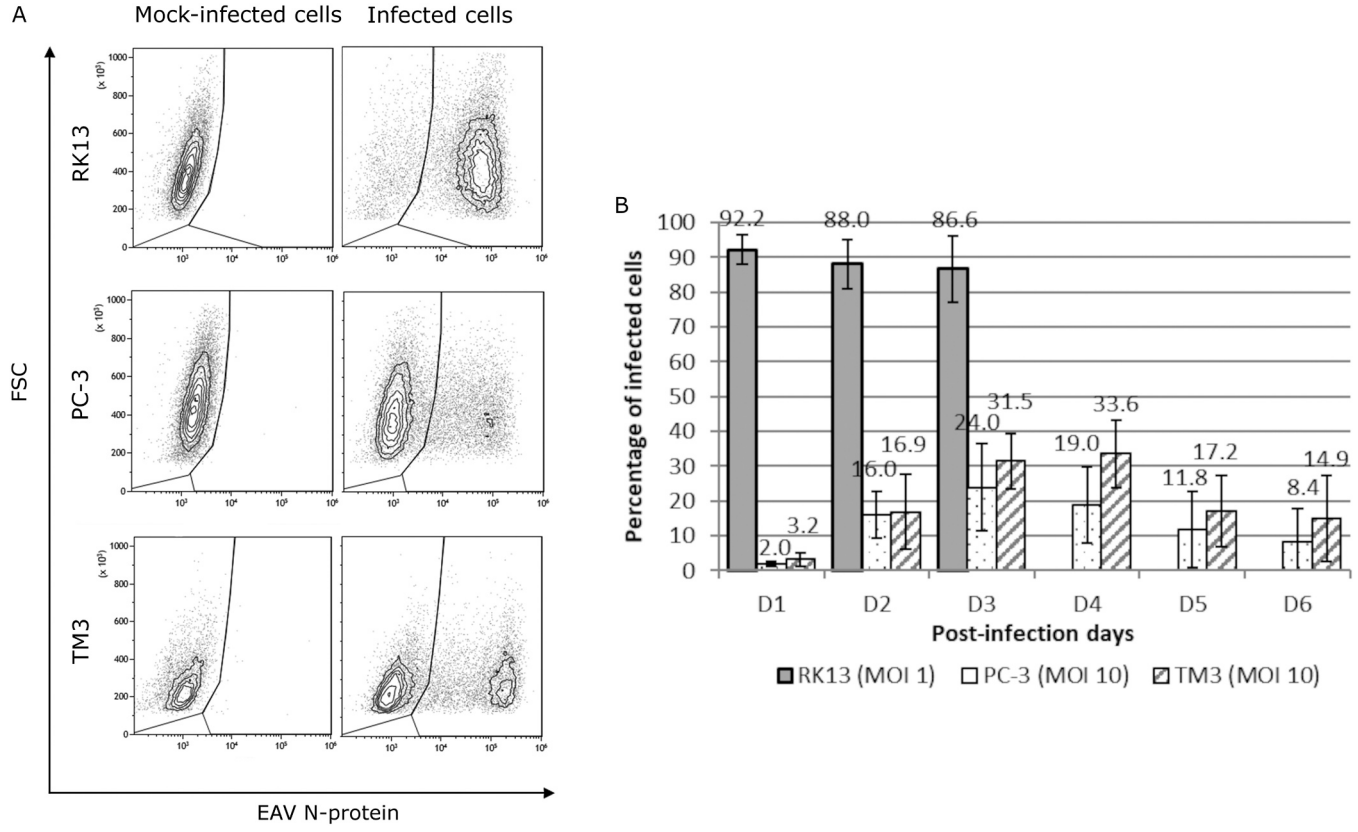

Fig. 4. Spreading of EAV in RK13, PC-3, and TM3 cell cultures. (A) Representative dot-plots for the gating of infected and non-infected cell populations at 1 dpi for the RK13 cell line and 3 dpi for the PC-3 and TM3 cell lines. (B) Percentages of infected cells obtained by flow cytometry until 6 dpi (D6). The medium was changed at 3 dpi for PC-3 and TM3 cells. Infected RK13 cells die after 3 dpi. Results are from 2 to 5 independent experiments (n = 2–4 for RK13 cells, n = 3–5 for PC-3 cells, n = 4–5 for TM3 cells) (mean +/- SD).

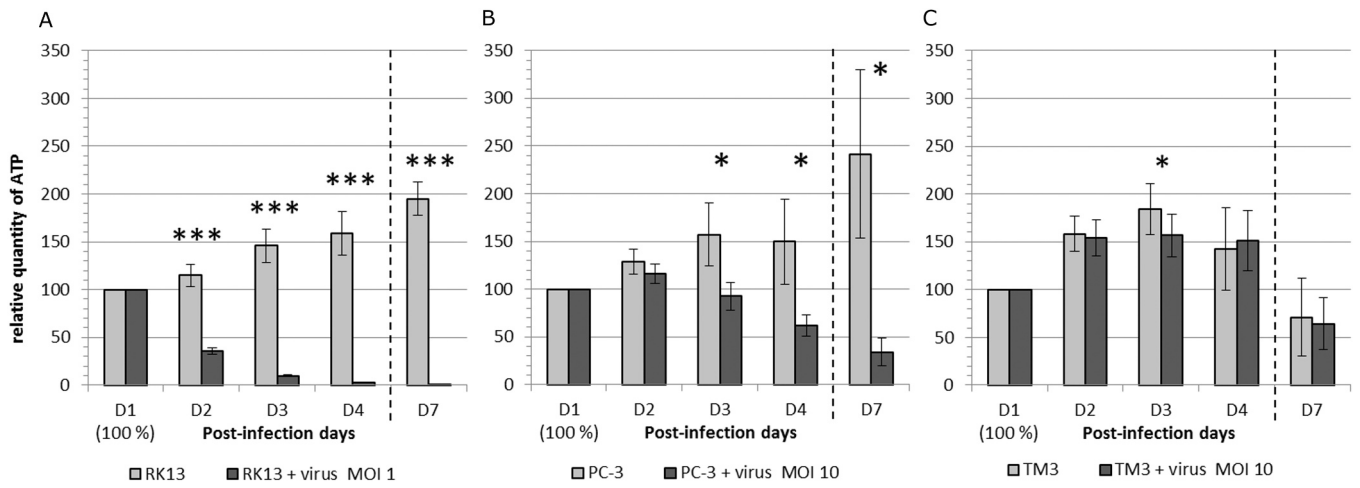

Fig. 5. Cell survival of the RK13, PC-3, and TM3 cell lines. CellTiter-Glo® assays from 1 dpi (D1) to 7 dpi (D7). For each condition, the luminescence signal obtained was normalized to the luminescence signal obtained at 1 dpi. Results are from 4 to 7 independent experiments (mean +/- SE). A one-tailed paired Student's *t*-test was performed comparing infected cell results to mock-infected cell results. * $p < 0.05$, ** $p < 0.01$, *** $p < 0.001$.

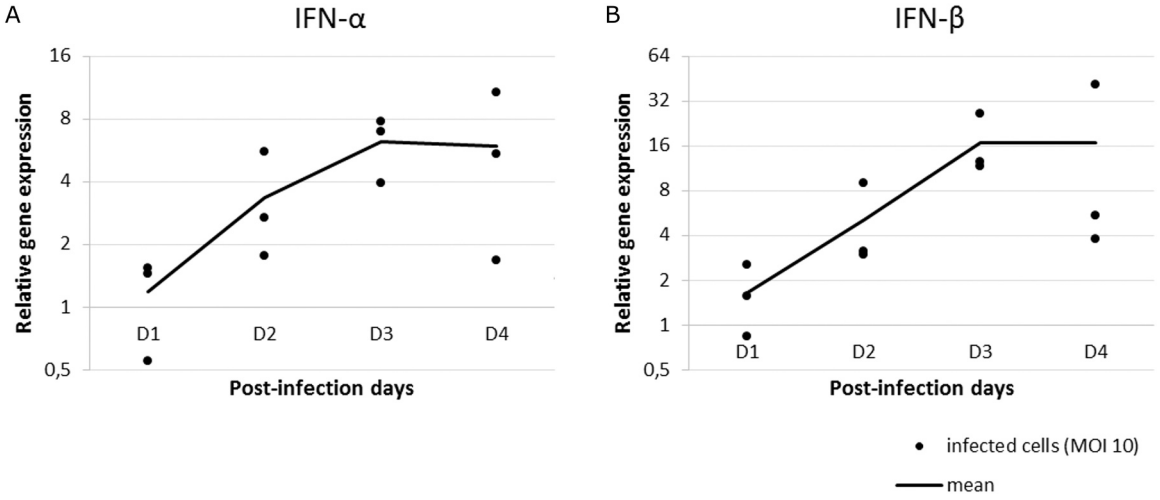

Fig. 6. Relative IFN-I gene expression in infected TM3 cells. Relative IFN-α (A) and IFN-β (B) gene expression was assessed from 1 dpi (D1) to 4 dpi (D4). Results are from 3 independent experiments. Data were normalized to actin gene expression using the $2^{-\Delta\Delta Ct}$ method. Each independent experiment is represented by a dot. The mean of the three experiments is shown by a line.

IFN-β gene expression were 0.9936 and 0.9715, respectively ($p = 0.0032$ and $p = 0.0143$, respectively).

3.5. Subcultures of EAV-infected TM3 cells

During the 7-day infections without subculturing, the percentage of infected TM3 cells reached about 30% after 3 dpi (Fig. 4B). Interestingly, subculturing (P1) infected TM3 cells at 1 or 2 dpi, this percentage of infection was over 70% (Fig. 7A). Subculturing cells at 3 dpi did not increase the percentage of infected cells: the infection rate remained at about 30% at 4 dpi (Fig. 7A).

Six assays were performed to try to maintain the infected TM3 cells in culture by subculturing them several times at 1:2, 1:5, 1:10, 1:20, or 1:100, every 1–6 days of culture (data not shown). Most of these assays could not be continued after 14 days of culture (2–4 passages). During one assay, we successfully maintained infected TM3 cells in culture for over 39 days (3 days after 14 passages) subculturing them at 1:2 the first time at 5 dpi and then every 2–3 days. However, although EAV was still present in the culture, the percentage of infected cells was remained low (0.7%) (Fig. 7B) and we decided to freeze them.

4. Discussion

Mechanisms involved in EAV persistence in the reproductive tract of some stallions remain largely unknown. Recent studies have shown EAV antigen-positive "T cells" (Carossino et al., 2017). However, the authors performed single staining of some "T cell markers", but not of TCR, the main marker of T cells, whereas they were staining outside lymphoid organs, whose structural organization is well-known. Unfortunately, it has been demonstrated in different species that myeloid cells, the first target of EAV, can express CD8, CD4, CD2, CD5, CXCL16, and even CD3 (Crawford et al., 1999; Gibbings and Befus, 2009; Rodriguez-Cruz et al., 2019; van Lieshout et al., 2009; Yin et al., 2017). NKT cells also express T cell markers. Moreover, no viral antigens were detected in "$CD4^+$ T cells" in the ampullae — the main tissue reservoir of EAV — of persistently infected stallions (Carossino et al., 2017), whereas Go et al. (2012) showed a majority of EAV susceptible cells are $CD4^+$ rather than $CD8^+$. Furthermore, viruses known to infect lymphocytes in humans, such as HIV, EBV, Measles virus, and HCV, are present in the whole organism, and especially in lymphoid organs, contrary to EAV.

It has been hypothesized that EAV induces lymphocyte homing in the stallion reproductive tract (Carossino et al., 2019, 2017), because, in

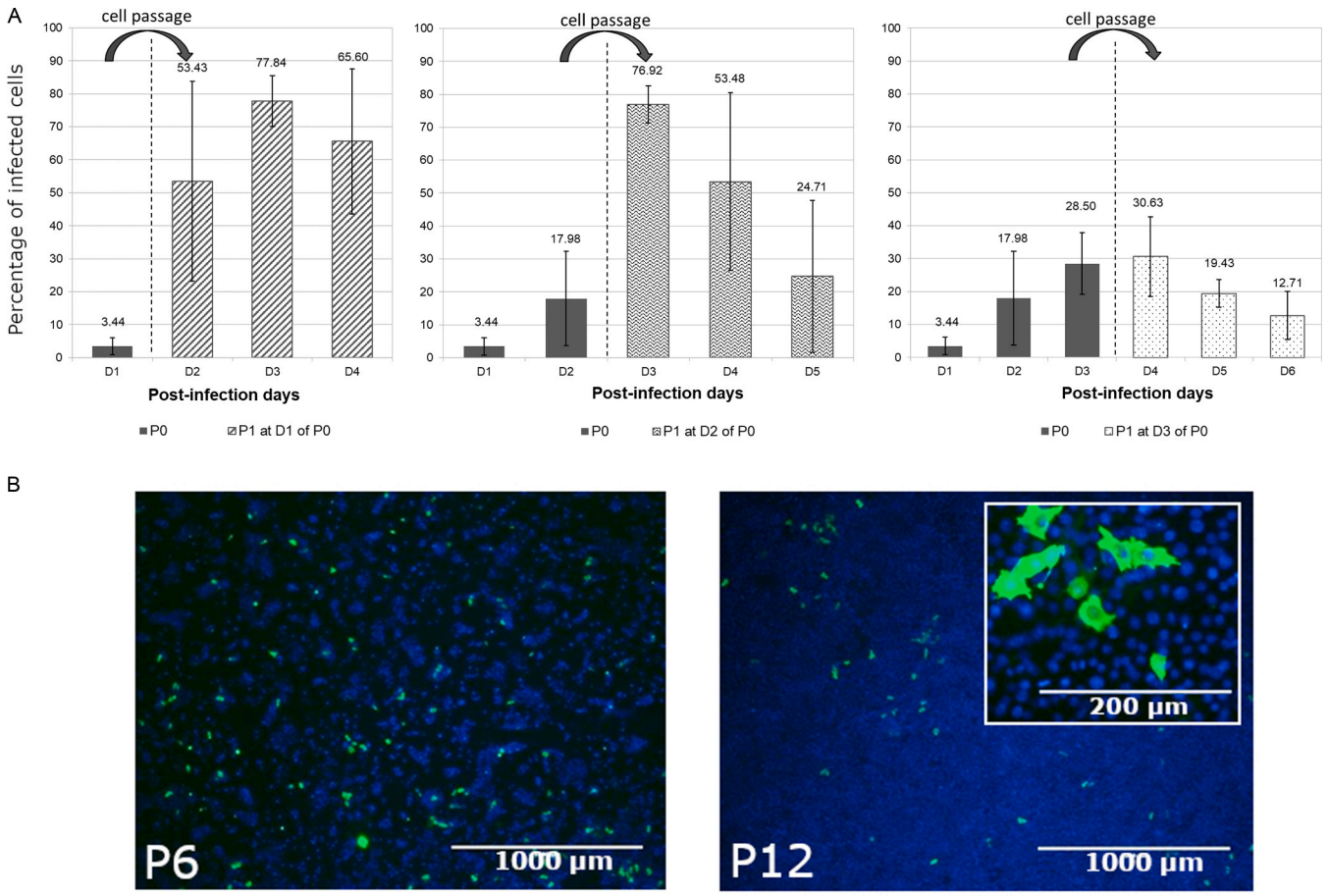

Fig. 7. Subcultures of EAV-infected TM3 cells. (A) Percentages of infected TM3 cells obtained by flow cytometry before (P0) and after (P1) cell passage. Infected TM3 cells were subcultured (P1) at 1:5 after 1, 2, or 3 dpi of P0 (n = 2). (B) Representative images of immunofluorescence staining on slides of EAV-infected TM3 cells successfully maintained in culture for over 39 days (EAV nucleocapsid [N] protein in green and cell nucleus in blue) after 6 subcultures (P6, 18 days of culture) and 12 subcultures (P12, 32 days of culture).

carrier stallions, infected lymphocytes are found only there (Carossino et al., 2017), and upregulation of CCL5, CXCL9, and CXCL10 expression was observed (Carossino et al., 2019). However, these three chemokines (CK) have all been described as inflammatory CK, not as homeostatic CK. Inflammatory CK are produced during infections to recruit circulating immune cells to the infection sites, whereas homeostatic CK, involved in homing processes, are constitutively and locally produced at steady state, without any infection occurring (Chen et al., 2018; Murphy and Weaver, 2016; Thelen and Uguccioni, 2016). After T cell recruitment to the infection sites, antigen recognition by effector T cells retains them there (Murphy and Weaver, 2016). Moreover, T cells are recruited until the pathogen is eliminated. EAV elimination occurs in the lungs, one portal of entry of EAV, but not in the reproductive tract of certain stallions. Therefore, the continuous recruitment of lymphocytes as potential susceptible host cells is not sufficient for viral persistence, contrary to what Carossino et al. (2017) suggested.

It has been demonstrated that EAV persistence depends on the presence of testosterone. The inhibitory effect of testosterone on the immune system does not explain this dependence, contrary to what Carossino et al. (2017) suggested, since not all viruses persist in the stallion reproductive tract. However, since the androgen receptor (AR) is also expressed in reproductive tract cells, testosterone may have a direct effect on EAV replication, especially because the AR is predominantly found in the glandular epithelia and scattered stromal cells (Carossino et al., 2019), and EAV has been found in stromal cells (fibrocytes and possibly macrophages) in the reproductive tract of persistently infected stallions (Carossino et al., 2017). For this reason, to study EAV testosterone-dependent persistence, we need an *in vitro* model of EAV infection of cells from the male reproductive tract that express the AR. Given that no cell lines derived from the stallion reproductive tract were available, we tested several cell lines from the male reproductive tract of other animal species. Among them, TM3 cells express the androgen receptor (Hwang et al., 2011) (characterized by ATCC, the supplier).

We described three distinct infection patterns: fully cytopathic (RK13, 92BR, and DDT1 MF-2 cells), without overt CPE at 3 dpi (PC-3 and TM3 cells), and non- or poorly permissive (ST, GC-1 spg, and LNCaP cells). At 0 dpi, there were 10-fold fewer viral genome copies in the supernatant of RK13 cells than in the other cell lines, probably because RK13 cells were infected at an MOI of 1, which is 10-fold lower than the MOI of 10 used for the other cell lines. At 2 dpi, viral production in RK13 and 92BR cells stopped and the virus infectivity decreased because most cells were infected and started to die due to viral infection. The delay in viral production observed in DDT1 MF-2 cells, compared with RK13 and 92BR cells, can be explained by a difference in the permissiveness to EAV infection of these cell lines. DDT1 MF-2 cells were much less infected at 1 dpi than were RK13 and 92BR cells, but reached the same percentage of infection as RK13 and 92BR cells at 3 dpi. These results indicate that viral entry is the key step for DDT1 MF-2 cell infection by EAV, whereas viral replication and the production of infectious viral particles did not seem to be inhibited within this cell line. Moreover, following the initial steps of infection, the virus spread rather quickly, suggesting viral adaptation to this cell line for infection.

The only cell lines that did not seem to be permissive to EAV infection were GC-1 spg cells and LNCaP cells. Nearly no viral genome copies

were detected in GC-1 spg cells upon infection, suggesting the possible absence of the receptor needed for viral entry. In LNCaP cells, no production of viral genome copies was detected, and no N proteins were detected. Thus, the detection of viral RNAs in the supernatants of LNCaP and GC-1 spg cells is due to the viral inoculum used for infection, and differences in the number of viral genome copies detected in the supernatants of LNCaP and GC-1 spg cells can be explained by the distinct infection protocols. LNCaP cells were left in presence of the virus for the length of the experiments to trigger infection, instead of the 5 h for the other cell lines, mainly to prevent LNCaP cells from detaching from the well bottoms. Also, viral RNAs detected within LNCaP cells may come from viral particles attached to the surface of LNCaP cells. Therefore, either LNCaP cells were not infected, or infection was aborted: the virus can enter the cells but cannot replicate. On the other hand, in ST cells, at 1 dpi, we detected less than 1% of infected cells by immunofluorescent staining on slides, whereas no infected cells were detected when analysed by flow cytometry. However, the virus was removed from the cell cultures at 5 h post-infection for flow cytometry experiments, whereas it was left with cells until fixation for immunofluorescent staining on slides. This modification in the protocol may explain the slight difference observed. Nevertheless, in both experiments, no ST cells were immunofluorescent-positive at 3 dpi, which seems to suggest that either ST cells eliminated the virus from the cell culture, or the virus killed the few infected cells. Alternatively, ST cells blocked the expression of the viral proteins.

Interestingly, the infection of TM3 cells without subculture led to a fully productive infection, with only 10-fold less infectious viral particles produced than with RK13 cells, although, at 3 dpi, around only 30% of TM3 cells were infected versus over 90% for RK13 cells. In comparison, the persistent EAV infection of Hela-H cells, a human female reproductive tract cell line, produced at 3 dpi around 10^5 PFU/mL with around only 20% of infected cells (Zhang et al., 2008), which is 500-fold less infectious viral particles than with their RK13 cells.

Interestingly, infection in TM3 cells without subculture did not modify cell viability compared with mock-infection of TM3 cells, except at 3 dpi that showed a slight difference. Because 3 dpi is the day with the highest percentage of infected cells, there may be lysis of only few cells or a slight slow-down in cell growth. However, in this case, there would be an equilibrium between cell lysis and cell growth, which may be due to faster growth of TM3 cells than of all the other cell lines tested in this study. Non-infected TM3 cells were subcultured twice a week at 1:20–1:30 versus 1:3 for PC-3 cells and 1:4–1:6 for RK13 cells. This fast growth may explain the decrease in metabolic activity in infected and mock-infected TM3 cells after 3 dpi when they are not subcultured for one week. Therefore, TM3 cell infection may mimic a chronic focal infection.

There are several mechanisms of *in vitro* viral persistence. Persistent infections can be non-productive, such as latent infections, in which the virus genome persists within cells either intra-chromosomally or extra-chromosomally, without production of viral particles (Boldogh et al., 1996; Mahy, 1985). The virus is transmitted vertically: its genome is replicated at the same time as the host cell genome and divided among daughter cells (Boldogh et al., 1996; Mahy, 1985). Persistent infections can also be productive, such as chronic infections, which include chronic diffuse infections and chronic focal infections. Chronic diffuse infections, also called steady-state infections, are infections in which most of cells are infected and viral particles are continuously produced without lysis of the host cells (Boldogh et al., 1996; Mahy, 1985). Chronic focal infections, also called carrier-state infections, have been described for positive-strand RNA viruses, such as group B coxsackieviruses (Crowell and Syverton, 1961; Pinkert et al., 2011; Rehren et al., 2013; Schnurr and Schmidt, 1984) and foot-and-mouth disease virus (FMDV) (de la Torre et al., 1988; de la Torre and Domingo, 1988; Martín-Acebes et al., 2010), for double-stranded RNA viruses, such as infectious pancreatic necrosis virus (IPNV) (García et al., 2011) and reovirus type 3 strain Dearing (T3D) (Dermody et al., 1993), and for DNA viruses, such as adenoviruses (Boldogh et al., 1996). Chronic focal infections are infections in which only a small proportion of cells is infected, from less than 1% to 70%, and releases high titres of infectious virus particles (10^3 to 10^9 PFU/mL) before being killed. The viruses thus released only infect a small proportion of the other cells (Crowell and Syverton, 1961; Dermody et al., 1993; García et al., 2011; Mahy, 1985; Pinkert et al., 2011; Rehren et al., 2013; Schnurr and Schmidt, 1984). However, through the equilibrium between cell growth and cell lysis, the global cell population survives, and is continuously infected, because the virus spreads through the medium or by direct contact between cells (Boldogh et al., 1996; Mahy, 1985; Pinkert et al., 2011). Thus, in certain circumstances, EAV infection in TM3 cells may lead to an equilibrium between cell growth and cell death. This was the case when infected TM3 cells were kept in culture for over 39 days with a low percentage of infected cells. This equilibrium between cell growth and cell death, in carrier-state cultures, is either permitted by the presence of inhibitory factors in the culture medium, such as interferons (Boldogh et al., 1996; García et al., 2011) and antibodies (Boldogh et al., 1996; Crowell and Syverton, 1961), or can be explained by a virus-host cell coevolution due to a difference in the susceptibility of the cells to the viral infection. Susceptibility differences can be due to mutations in the "viral" receptor, to a reduction in its expression (Pinkert et al., 2011), or to an intracellular blocking of the virus uptake process (Dermody et al., 1993) or of virus replication (de la Torre et al., 1988). Because we observed overexpression of the IFN-α and IFN-β genes in our TM3 cell model of EAV infection, interferons may play a role in this carrier-state like infection. Despite the capacity of some EAV non-structural proteins (nsp1, nsp2, and nsp11) to decrease the induction of IFN-β gene expression (Go et al., 2014; Han et al., 2014), in our TM3 cell infection model, EAV infection did not prevent IFN-I gene expression. IFN-α and IFN-β gene expression levels were at their maximum at 3 dpi in the infection of TM3 cells without subculture and this was correlated with the highest percentage of infected cells. This production of interferons may explain why the production of viral particles also peaked at 3 dpi, and why the percentage of infected cells did not increase when infected TM3 cells were subcultured at 3 dpi, whereas it did increase when infected TM3 cells were subcultured at 1 or 2 dpi. When that virus replication-cell survival equilibrium is out of balance, it can lead either to the elimination of the virus (Schnurr and Schmidt, 1984) or to the death of the cell culture. The imbalance in the equilibrium brought about by the excessive virus replication compared with cell growth can depend on the initial MOI and on the virulence of the strain. For example, one study (Rehren et al., 2013) showed that the coxsackievirus B3 (CVB3) Nancy strain at an MOI of 0.01–0.1 TCID50/cell leads to a persistent carrier-state infection, whereas another strain (CVB3 PD, a strain derived from CVB3 Nancy) at an MOI of 1–100 TCID50/cell leads to acute lytic infection. Moreover, another study (Pinkert et al., 2011) showed that the HL-1 mouse atrial cardiomyocyte cell line infected at an MOI of 10, 1, or 0.1 does not present overt cell lysis at 3 dpi, but after having been subcultured at 2 dpi, only the cells infected at an MOI of 0.1 are able to grow to a confluent cell monolayer. In an older study (Crowell and Syverton, 1961), at the 7^{th} passage, the infected cells did not grow to a confluent cell monolayer, but some infected cells were maintained in culture for 9 months without any passages. Likewise, our infected TM3 cells subcultured at 1:5 at 1 or 2 dpi showed an increase in the percentage of infected cells and did not grow to a confluent cell monolayer, whereas infected TM3 cells could be kept in culture for over 39 days when they were subcultured at 1:2 the first time at 5 dpi and then every 2–3 days.

5. Conclusion

In summary, we established an *in vitro* model of EAV infection in a male reproductive tract cell line. Among the several mechanisms of *in vitro* viral persistence, EAV TM3 cell infection is a chronic focal infection. This is the first chronic focal EAV infection of a male reproductive tract cell line. The EAV TM3 cell infection may be an interesting model

for the study of host-pathogen interactions, because this infection can be maintained at least 7 days in culture, without any subculture, whereas infected RK13 cells can be kept only 2 days in culture before dying. Moreover, for short-term studies, the percentage of infected TM3 cells can be increased by subculturing them at 1 or 2 dpi. Infected TM3 cells can also be subcultured for over 39 days, but in this case the percentage of infected cells remains low. TM3 cell infection can help to better understand the mechanisms involved in EAV persistence in the stallion reproductive tract, notably the possible direct impact of testosterone on EAV replication.

Funding

This study was supported by ANSES (French Agency for Food, Environmental and Occupational Health and Safety), the Normandy Regional Council, and the IFCE (French Institute for Horse and Horse Riding).

CRediT authorship contribution statement

Lydie Martín-Faivre: Investigation, Formal analysis, Visualization, Writing – original draft, Writing – review & editing. **Delphine Gaudaire:** Investigation, Writing – review & editing. **Claire Laugier:** Conceptualization, Writing - review & editing. **Hélène Bouraïma-Lelong:** Conceptualization, Writing - review & editing. **Stéphan Zientara:** Conceptualization, Writing - review & editing. **Aymeric Hans:** Supervision, Conceptualization, Writing - review & editing.

Declaration of Competing Interest

The authors declare that they have no known competing financial interests or personal relationships that could have appeared to influence the work reported in this paper.

Data Availability

Data will be made available on request.

Acknowledgments

We are grateful to Marilyne Guillamin and the flow cytometry platform of the SF 4206 ICORE, welcomed inside the BioTICLA Unit (INSERM, U1199), in the Comprehensive Cancer Center François Baclesse, Unicancer, Caen, France.

References

Alimirah, F., Chen, J., Basrawala, Z., Xin, H., Choubey, D., 2006. DU-145 and PC-3 human prostate cancer cell lines express androgen receptor: implications for the androgen receptor functions and regulation. FEBS Lett. 580, 2294–2300. https://doi.org/10.1016/j.febslet.2006.03.041.

Balasuriya, U.B.R., Go, Y.Y., MacLachlan, N.J., 2013. Equine arteritis virus. Vet. Microbiol 167, 93–122. https://doi.org/10.1016/j.vetmic.2013.06.015.

Balasuriya, U.B.R., Leutenegger, C.M., Topol, J.B., McCollum, W.H., Timoney, P.J., MacLachlan, N.J., 2002. Detection of equine arteritis virus by real-time TaqMan reverse transcription-PCR assay. J. Virol. Methods 101, 21–28. https://doi.org/10.1016/s0166-0934(01)00416-5.

Boldogh, I., Albrecht, T., Porter, D.D., 1996. Persistent Viral Infections., in: Baron, S. (Ed.), Medical Microbiology. University of Texas Medical Branch at Galveston, Galveston (TX).

Burger, D., Janett, F., Vidament, M., Stump, R., Fortier, G., Imboden, I., Thun, R., 2006. Immunization against GnRH in adult stallions: effects on semen characteristics, behaviour, and shedding of equine arteritis virus. Anim. Reprod. Sci. 94, 107–111. https://doi.org/10.1016/j.anireprosci.2006.03.098.

Carossino, M., Dini, P., Kalbfleisch, T.S., Loynachan, A.T., Canisso, I.F., Cook, R.F., Timoney, P.J., Balasuriya, U.B.R., 2019. Equine arteritis virus long-term persistence is orchestrated by CD8+ T lymphocyte transcription factors, inhibitory receptors, and the CXCL16/CXCR6 axis. PLoS Pathog. 15, e1007950 https://doi.org/10.1371/journal.ppat.1007950.

Carossino, M., Loynachan, A.T., Canisso, I.F., Cook, R.F., Campos, J.R., Nam, B., Go, Y.Y., Squires, E.L., Troedsson, M.H.T., Swerczek, T., Del Piero, F., Bailey, E., Timoney, P. J., Balasuriya, U.B.R., 2017. Equine arteritis virus has specific tropism for stromal cells and $CD8^+$ T and $CD21^+$ B lymphocytes but not for glandular epithelium at the primary site of persistent infection in the stallion reproductive tract. J. Virol. 91 https://doi.org/10.1128/JVI.00418-17.

Chen, K., Bao, Z., Tang, P., Gong, W., Yoshimura, T., Wang, J.M., 2018. Chemokines in homeostasis and diseases. Cell Mol. Immunol. 15, 324–334. https://doi.org/10.1038/cmi.2017.134.

Crawford, K., Gabuzda, D., Pantazopoulos, V., Xu, J., Clement, C., Reinherz, E., Alper, C. A., 1999. Circulating CD2+ monocytes are dendritic cells. J. Immunol. 163, 5920–5928. https://doi.org/10.4049/jimmunol.163.11.5920.

Crowell, R.L., Syverton, J.T., 1961. The mammalian cell-virus relationship. VI. Sustained infection of HeLa cells by Coxsackie B3 virus and effect on superinfection. J. Exp. Med. 113, 419–435. https://doi.org/10.1084/jem.113.2.419.

de la Torre, J.C., Domingo, E., 1988. Minimum number of cells required for reconstitution of a foot-and-mouth disease virus-carrier cell culture. Microbiologia 4, 161–166.

de la Torre, J.C., Martínez-Salas, E., Diez, J., Villaverde, A., Gebauer, F., Rocha, E., Dávila, M., Domingo, E., 1988. Coevolution of cells and viruses in a persistent infection of foot-and-mouth disease virus in cell culture. J. Virol. 62, 2050–2058. https://doi.org/10.1128/JVI.62.6.2050-2058.1988.

Dermody, T.S., Nibert, M.L., Wetzel, J.D., Tong, X., Fields, B.N., 1993. Cells and viruses with mutations affecting viral entry are selected during persistent infections of L cells with mammalian reoviruses. J. Virol. 67, 2055–2063. https://doi.org/10.1128/JVI.67.4.2055-2063.1993.

Fukunaga, Y., Wada, R., Kamada, M., Kumanomido, T., Akiyama, Y., 1984. Tentative preparation of an inactivated virus vaccine for equine viral arteritis. Bull. Equine Res. Inst. 1984, 56–64. https://doi.org/10.11535/jes1977.1984.56.

García, I., Galiana, A., Falcó, A., Estepa, A., Perez, L., 2011. Characterization of an infectious pancreatic necrosis (IPN) virus carrier cell culture with resistance to superinfection with heterologous viruses. Vet. Microbiol. 149, 48–55. https://doi.org/10.1016/j.vetmic.2010.10.017.

Gibbings, D., Befus, A.D., 2009. CD4 and CD8: an inside-out coreceptor model for innate immune cells. J. Leukoc. Biol. 86, 251–259. https://doi.org/10.1189/jlb.0109040.

Go, Y.Y., Bailey, E., Timoney, P.J., Shuck, K.M., Balasuriya, U.B.R., 2012. Evidence that in vitro susceptibility of CD3+ T lymphocytes to equine arteritis virus infection reflects genetic predisposition of naturally infected stallions to become carriers of the virus. J. Virol. 86, 12407–12410. https://doi.org/10.1128/JVI.01698-12.

Go, Y.Y., Li, Y., Chen, Z., Han, M., Yoo, D., Fang, Y., Balasuriya, U.B.R., 2014. Equine arteritis virus does not induce interferon production in equine endothelial cells: identification of nonstructural protein 1 as a main interferon antagonist. Biomed. Res. Int. 2014, 420658 https://doi.org/10.1155/2014/420658.

Golnik, W., Michalska, Z., Michalak, T., 1981. Natural equine viral arteritis in foals. Schweiz Arch. Tierheilkd. 123, 523–533. https://doi.org/10.5169/seals-593411.

Han, M., Kim, C.Y., Rowland, R.R.R., Fang, Y., Kim, D., Yoo, D., 2014. Biogenesis of non-structural protein 1 (nsp1) and nsp1-mediated type I interferon modulation in arteriviruses. Virology 458–459, 136–150. https://doi.org/10.1016/j.virol.2014.04.028.

Holyoak, G.R., Little, T.V., McCollum, W.H., Timoney, P.J., 1993. Relationship between onset of puberty and establishment of persistent infection with equine arteritis virus in the experimentally infected colt. J. Comp. Pathol. 109, 29–46. https://doi.org/10.1016/S0021-9975(08)80238-1.

Hwang, T.I.S., Liao, T.-L., Lin, J.-F., Lin, Y.-C., Lee, S.-Y., Lai, Y.-C., Kao, S.-H., 2011. Low-dose testosterone treatment decreases oxidative damage in TM3 Leydig cells. Asian J. Androl. 13, 432–437. https://doi.org/10.1038/aja.2010.159.

Janett, F., Stump, R., Burger, D., Thun, R., 2009. Suppression of testicular function and sexual behavior by vaccination against GnRH (Equity) in the adult stallion. Anim. Reprod. Sci. 115, 88–102. https://doi.org/10.1016/j.anireprosci.2008.11.011.

Konishi, S., Akashi, H., Sentsui, H., Ogata, M., 1975. Studies on equine viral arteritis. I. Characterization of the virus and trial survey on antibody with vero cell cultures. Nihon Juigaku Zasshi 37, 259–267. https://doi.org/10.1292/jvms1939.37.5_259.

Li, T., Hu, J., He, G.-H., Li, Y., Zhu, C.-C., Hou, W.-G., Zhang, S., Li, W., Zhang, J.-S., Wang, Z., Liu, X.-P., Yao, L.-B., Zhang, Y.-Q., 2012. Up-regulation of NDRG2 through nuclear factor-kappa B is required for Leydig cell apoptosis in both human and murine infertile testes. Biochim Biophys. Acta 1822, 301–313. https://doi.org/10.1016/j.bbadis.2011.11.013.

Little, T.V., Holyoak, G.R., McCollum, W.H., Timoney, P.J., 1992. Output of equine arteritis virus from persistently infected carrier stallions is testosterone dependent. Proc. 6th Int. Conf. Equine Infect. Dis., Camb. 1991, 225–229.

Lu, Z., Zhang, J., Huang, C.M., Go, Y.Y., Faaberg, K.S., Rowland, R.R.R., Timoney, P.J., Balasuriya, U.B.R., 2012. Chimeric viruses containing the N-terminal ectodomains of GP5 and M proteins of porcine reproductive and respiratory syndrome virus do not change the cellular tropism of equine arteritis virus. Virology 432, 99–109. https://doi.org/10.1016/j.virol.2012.05.022.

Ma, C., Song, H., Yu, L., Guan, K., Hu, P., Li, Y., Xia, X., Li, J., Jiang, S., Li, F., 2016. miR-762 promotes porcine immature Sertoli cell growth via the ring finger protein 4 (RNF4) gene. Sci. Rep. 6, 32783. https://doi.org/10.1038/srep32783.

Mahy, B.W.J., 1985. Strategies of virus persistence. Br. Med. Bull. 41, 50–55. https://doi.org/10.1093/oxfordjournals.bmb.a072024.

Martín-Acebes, M.A., Herrera, M., Armas-Portela, R., Domingo, E., Sobrino, F., 2010. Cell density-dependent expression of viral antigens during persistence of foot-and-mouth disease virus in cell culture. Virology 403, 47–55. https://doi.org/10.1016/j.virol.2010.04.005.

McCollum, W.H., Little, T.V., Timoney, P.J., Swerczek, T.W., 1994. Resistance of castrated male horses to attempted establishment of the carrier state with equine arteritis virus. J. Comp. Pathol. 111, 383–388. https://doi.org/10.1016/S0021-9975(05)80096-9.

Metz, G.E., Serena, M.S., Panei, C.J., Nosetto, E.O., Echeverria, M.G., 2014. The equine arteritis virus isolate from the 2010 Argentinian outbreak. Rev. Sci. Tech. 33, 937–946. https://doi.org/10.20506/rst.33.3.2331.

Murphy, K., Weaver, C., 2016. Janeway's Immunobiology. W.W. Norton.

Neu, S.M., Timoney, P.J., McCollum, W.H., 1988. Persistent infection of the reproductive tract in stallions experimentally infected with equine arteritis virus. In Equine Infectious Diseases V: Proceedings of the Fifth International Conference on Equine Infectious Diseases, Lexington, 1987, Edited by D.G. Powell. The University Press of Kentucky, Lexington. 149–154.

Pinkert, S., Klingel, K., Lindig, V., Dörner, A., Zeichhardt, H., Spiller, O.B., Fechner, H., 2011. Virus-host coevolution in a persistently coxsackievirus B3-infected cardiomyocyte cell line. J. Virol. 85, 13409–13419. https://doi.org/10.1128/JVI.00621-11.

Pronost, S., Pitel, P.H., Miszczak, F., Legrand, L., Marcillaud-Pitel, C., Hamon, M., Tapprest, J., Balasuriya, U.B.R., Freymuth, F., Fortier, G., 2010. Description of the first recorded major occurrence of equine viral arteritis in France. Equine Vet. J. 42, 713–720. https://doi.org/10.1111/j.2042-3306.2010.00109.x.

Rehren, F., Ritter, B., Dittrich-Breiholz, O., Henke, A., Lam, E., Kati, S., Kracht, M., Heim, A., 2013. Induction of a broad spectrum of inflammation-related genes by Coxsackievirus B3 requires Interleukin-1 signaling. Med Microbiol Immunol. 202, 11–23. https://doi.org/10.1007/s00430-012-0245-2.

Rodriguez-Cruz, A., Vesin, D., Ramon-Luing, L., Zuñiga, J., Quesniaux, V.F.J., Ryffel, B., Lascurain, R., Garcia, I., Chávez-Galán, L., 2019. $CD3^+$ macrophages deliver proinflammatory cytokines by a CD3- and transmembrane TNF-Dependent pathway and are increased at the BCG-Infection site. Front Immunol 10, 2550. https://doi.org/10.3389/fimmu.2019.02550.

Sarkar, S., Bailey, E., Go, Y.Y., Cook, R.F., Kalbfleisch, T., Eberth, J., Chelvarajan, R.L., Shuck, K.M., Artiushin, S., Timoney, P.J., Balasuriya, U.B.R., 2016. Allelic Variation in CXCL16 Determines CD3+ T lymphocyte susceptibility to equine arteritis virus infection and establishment of long-term carrier state in the stallion. PLoS Genet 12, e1006467. https://doi.org/10.1371/journal.pgen.1006467.

Schnurr, D.P., Schmidt, N.J., 1984. Persistent infection of mouse fibroblasts with coxsackievirus. Arch. Virol. 81, 91–101. https://doi.org/10.1007/BF01309299.

Shen, X., Liu, L., Yin, F., Ma, H., Zou, S., 2012. Effect of dehydroepiandrosterone on cell growth and mitochondrial function in TM-3 cells. Gen. Comp. Endocrinol. 177, 177–186. https://doi.org/10.1016/j.ygcen.2012.03.007.

Shin, S., Kim, T.-D., Jin, F., van Deursen, J.M., Dehm, S.M., Tindall, D.J., Grande, J.P., Munz, J.-M., Vasmatzis, G., Janknecht, R., 2009. Induction of prostatic intraepithelial neoplasia and modulation of androgen receptor by ETS variant 1/ETS-related protein 81. Cancer Res 69, 8102–8110. https://doi.org/10.1158/0008-5472.CAN-09-0941.

Siddell, S.G., Walker, P.J., Lefkowitz, E.J., Mushegian, A.R., Adams, M.J., Dutilh, B.E., Gorbalenya, A.E., Harrach, B., Harrison, R.L., Junglen, S., Knowles, N.J., Kropinski, A.M., Krupovic, M., Kuhn, J.H., Nibert, M., Rubino, L., Sabanadzovic, S., Sanfaçon, H., Simmonds, P., Varsani, A., Zerbini, F.M., Davison, A.J., 2019. Additional changes to taxonomy ratified in a special vote by the International Committee on Taxonomy of Viruses (October 2018). Arch. Virol. 164, 943–946. https://doi.org/10.1007/s00705-018-04136-2.

Stout, T.A.E., 2005. Modulating reproductive activity in stallions: a review. Anim. Reprod. Sci. 89, 93–103. https://doi.org/10.1016/j.anireprosci.2005.06.015.

Thelen, M., Uguccioni, M., 2016. Function of Chemokines and Their Receptors in Immunity. In: Ratcliffe, M.J.H. (Ed.), Encyclopedia of Immunobiology. Academic Press, Oxford, pp. 572–578. https://doi.org/10.1016/B978-0-12-374279-7.10008-6.

van Lieshout, A.W.T., van der Voort, R., Toonen, L.W.J., van Helden, S.F.G., Figdor, C.G., van Riel, P.L.C.M., Radstake, T.R.D.J., Adema, G.J., 2009. Regulation of CXCL16 expression and secretion by myeloid cells is not altered in rheumatoid arthritis. Ann. Rheum. Dis. 68, 1036–1043. https://doi.org/10.1136/ard.2007.086611.

Wada, R., Fukunaga, Y., Kanemaru, T., Kondo, T., 1996. Histopathological and immunofluorescent studies on transplacental infection in experimentally induced abortion by equine arteritis virus. Zent. Vet. B 43, 65–74. https://doi.org/10.1111/j.1439-0450.1996.tb00290.x.

Wang, J., Bao, B., Meng, F., Deng, S., Feng, J., Dai, H., Xu, H., Zhao, Q., Li, H., Wang, B., 2021. In vitro and in vivo investigation of the therapeutic mechanism of Lycium chinense and Cuscutae Semen on oligoasthenozoospermia. Andrologia 53, e14014. https://doi.org/10.1111/and.14014.

Wu, H., Shi, L., Wang, Q., Cheng, L., Zhao, X., Chen, Q., Jiang, Q., Feng, M., Li, Q., Han, D., 2016. Mumps virus-induced innate immune responses in mouse Sertoli and Leydig cells. Sci. Rep. 6, 19507. https://doi.org/10.1038/srep19507.

Yin, X., Yu, H., Jin, X., Li, J., Guo, H., Shi, Q., Yin, Z., Xu, Y., Wang, X., Liu, R., Wang, S., Zhang, L., 2017. Human Blood CD1c+ dendritic cells encompass CD5high and CD5low subsets that differ significantly in phenotype, gene expression, and functions. J. Immunol. 198, 1553–1564. https://doi.org/10.4049/jimmunol.1600193.

Zhang, J., Timoney, P.J., MacLachlan, N.J., McCollum, W.H., Balasuriya, U.B.R., 2008. Persistent equine arteritis virus infection in HeLa cells. J. Virol. 82, 8456–8464. https://doi.org/10.1128/JVI.01249-08.